John von Neumann Institute for Computing

NIC

Realistic Description of TTF-TCNQ – a Strongly Correlated Organic Metal

A. Dolfen, E. Koch

Realistic Description of TTF-TCNQ – a Strongly Correlated Organic Metal

Andreas Dolfen and Erik Koch

Institut für Festkörperforschung, Forschungszentrum Jülich, 52425 Jülich, Germany
E-mail: {a.dolfen, e.koch}@fz-juelich.de

Understanding the physics of strongly correlated materials is one of the grand challenges in condensed-matter physics. Simple approximations such as the local density approximation fail, due to the importance of the Coulomb repulsion between localized electrons. Instead we have to resort to non-perturbative many-body techniques. Such calculations are, however, only feasible for quite small model systems. This means that the full Hamiltonian of a real material has to be approximated by a model Hamiltonian comprising only the most important electronic degrees of freedom, while the effect of all other electrons can merely be included in an average way in form of parameters. In this work we describe how to calculate those parameters for the one-dimensional organic metal TTF-TCNQ. Having constructed the Hamiltonian we calculate the ground state and dynamical properties with the Lanczos method. This method is limited by the available main memory. We show how to make efficient use of the memory and computational power of the massively parallel BlueGene/L system for such calculations. To gain high-resolution angular-resolved spectral functions we employ cluster perturbation theory (CPT) which helps identifying signatures of spin-charge separation also found experimentally in TTF-TCNQ. Increasing the nearest neighbour interaction is studied using a periodic version of CPT (kCPT).

1 Motivation

Essentially all of condensed matter physics is described by the non-relativistic Schrödinger equation $i\hbar\frac{\partial}{\partial t}|\Psi\rangle = H|\Psi\rangle$, with the Hamiltonian

$$H = -\sum_{\alpha=1}^{N_n}\frac{\vec{P}_\alpha^2}{2M_\alpha} - \sum_{j=1}^{N_e}\frac{\vec{p}_j^2}{2m} - \sum_{j=1}^{N_e}\sum_{\alpha=1}^{N_n}\frac{Z_\alpha e^2}{|\vec{r}_j - \vec{R}_\alpha|} + \sum_{j<k}^{N_e}\frac{e^2}{|\vec{r}_j - \vec{r}_k|} + \sum_{\alpha<\beta}^{N_n}\frac{Z_\alpha Z_\beta e^2}{|\vec{R}_\alpha - \vec{R}_\beta|}$$

where Z_α is the atomic number, M_α the mass, $\vec{R}_\alpha$ the position and $\vec{P}_\alpha$ the momentum of nucleus α. $\vec{p}_j$ and $\vec{r}_j$ denote the jth electron's momentum and position and N_e, N_n the number of electrons and nuclei, respectively. To accurately describe materials of technological interest and design new ones with superior properties, all we have to do is solve this equation. There is, however, a severe problem which makes a brute-force approach to the many-body Schrödinger equation infeasible. To illustrate this, let us consider a single iron atom. With its 26 electrons the total electronic wave function depends on 26 times 3 spatial coordinates. Thus, even without spin, specifying the electronic wave function on a hypercubic grid with merely 10 points per coordinate, we would have to store 10^{78} numbers. This is impossible in practice: Even if we could store a number in a single hydrogen atom, the required memory would weight 10^{51} kg – far more than our home-galaxy, the milky way.

Still, the quantitative description of solids is not an entirely hopeless enterprise. Even though an exact treatment is a practical impossibility, there are successful approximations that work for wide classes of materials. The most prominent examples are approximations to density functional theory.[1] They effectively map the hard many-body problem to
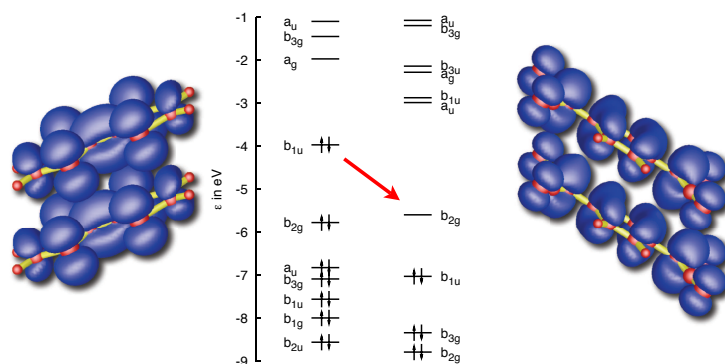
Figure 1. The molecular metal TTF-TCNQ. Centre: molecular levels of the isolated molecules; left: two TTF molecules with the electron density of their highest occupied molecular orbital (HOMO); right: TCNQ with the electron density of the lowest unoccupied molecular orbital (LUMO). The red arrow denotes the charge transfer of 0.6 electrons from the TTF-HOMO to the TCNQ-LUMO.

an effective single-particle problem that can be efficiently solved numerically. Essential to these approximations is that the Coulomb repulsion is described on a mean-field level. Such an approximation fails, however, to capture the physics in systems with strong correlations. In these systems the Coulomb repulsion between the electrons is so strong that the motion of a single electron depends on the position of all the others. The electrons thus lose their individuality and the single-electron picture breaks down. To accurately model this, we have to solve the many-electron problem exactly. Clearly we cannot do this for the full Hamiltonian. Instead, we consider a simplified Hamiltonian, which describes only those electrons that are essential to the correlation effects.[2] In this work we find the model Hamiltonian for the one-dimensional organic metal TTF-TCNQ and solve it numerically.

As shown in figure 1, TTF and TCNQ are stable molecules with completely filled molecular orbitals. The highest molecular orbital (HOMO) of TTF is, however, significantly higher in energy than the lowest unoccupied molecular orbital (LUMO) of TCNQ. Thus in a crystal of TTF and TCNQ, charge is transferred from the TTF-HOMO to the TCNQ-LUMO. This leads to partially filled bands and thus metallic behaviour. In the TTF-TCNQ crystal, like molecules are stacked on top of each other. Electrons can move along these stacks, while hopping between different stacks is extremely weak. Thus the material is quasi one-dimensional.

As pointed out above, we cannot treat all the electrons in the molecular solid. Instead, we focus our efforts on the most important electronic states: the partially filled TTF-HOMO and TCNQ-LUMO. The effects of the other electrons are included by considering their screening effects.[3] The simplest model Hamiltonian which captures both effects, the itinerancy of the electrons as well as the strong Coulomb interaction is the Hubbard model. We present a slightly extended Hubbard model, it reads

$$H = -\sum_{\sigma, i \neq j} t_{ij} c_{i\sigma}^{\dagger} c_{j\sigma} + U \sum_i n_{i\uparrow} n_{i\downarrow} + V \sum_{<ij>} n_i n_j \, . \qquad (1)$$

238

The first term gives the kinetic energy, where t_{ij} is the amplitude for an electron to hop from the molecule at site i to lattice site j. Note that hopping does not change the spin σ. The second and third terms represent the Coulomb repulsion between electrons in the same molecular orbital (second term) and in neighbouring molecular orbitals (third term). The values of U and V determine the strength of the Coulomb repulsion for two electrons in the same molecular orbital or neighbouring ones, respectively. In the next section we will address the problem of calculating those parameters.

Since the Hamiltonian does neither change the number of electrons nor their spin, we need to consider (1) only on Hilbert spaces with a fixed number of electrons of spin up $N_\uparrow$ and spin down $N_\downarrow$. For a finite system of L orbitals there are $\binom{L}{N_\sigma}$ different ways to arrange N_σ electrons of spin σ. Thus the dimension of the Hilbert space is given by $\binom{L}{N_\uparrow} \cdot \binom{L}{N_\downarrow}$. Even though we significantly simplified the problem, we still have to face the many-body problem: increasing system size, the dimension of the Hilbert space increases steeply. A system with 20 orbitals and 10 electrons of either spin already contains more than 34 billion (34 134 779 536) different configurations. Storing a single many-body state for this system takes about 254 GB.

2 Calculation of Parameters for a Realistic Description

For a realistic description of TTF-TCNQ we employ all-electron DFT using the Perdew-Burke-Ernzerhof functional.[4] We start with the hopping matrix elements t along stacks of like molecules. Due to the relatively small overlap of the molecular wave functions the description in terms of the tight-binding model is a good approximation, for the same reason nearest neighbour hopping suffices. Similar to atomic energy levels splitting in bonding and anti-bonding levels when forming diatomic homonuclear molecules the molecular energy levels of isolated molecules split when two molecules approach one another. From this bonding and anti-bonding splitting for a pair of like molecules we obtain the absolute value of the hopping parameter. Let ν denote the molecular level for which we want to calculate the hopping parameter, here either the HOMO of TTF or the LUMO of TCNQ, and ε_ν its molecular energy. In a specific dimer with states $|\phi_\nu^x\rangle$, where $x = A, B$ distinguishes the two molecules, the tight-binding Hamiltonian reads

$$H_\nu^{\mathrm{TBA}} = \begin{pmatrix} \varepsilon_\nu & -t^\nu \\ -t^\nu & \varepsilon_\nu \end{pmatrix} . \tag{2}$$

Diagonalizing yields the symmetric/anti-symmetric state, i.e. $|\varphi_\nu^{s/a}\rangle = \frac{1}{\sqrt{2}}\left(|\phi_\nu^A\rangle \pm |\phi_\nu^B\rangle\right)$, with the corresponding energies, i.e. $|\epsilon_\nu^{s/a}\rangle = \varepsilon_\nu \mp t^\nu$. From this we obtain the absolute value of the hopping parameter by dividing the splitting $|\Delta\varepsilon^\nu| = 2|t^\nu|$ of the molecular energy levels by two. The sign of t^ν, however, is not directly accessible by this method. It can be derived from the symmetry of the dimer wavefunctions. If the bonding orbital (the lower one in energy) is symmetric ($\left|\varphi_\nu^{s/a}\right\rangle$) then t_ν is positive. And correspondingly if the lower one is antisymmetric, t is negative. For TTF-TCNQ we obtain: $t = -0.15$ eV for TTF and 0.18 eV for TCNQ.

The Coulomb parameters are harder to determine due to the screening processes inside the crystal. We start with the bare Coulomb integrals of the molecular orbital ν for two

	TTF	TCNQ		TTF	TCNQ
U_{bare}	5.9	5.4	V_{bare}	3.1	2.9
U_0	4.7	4.3	V_0	2.9	2.8
U	2	1.7	V	1	0.9

Table 1. Hubbard parameters for TTF-TCNQ. U_{bare} is the direct Coulomb integral, U_0 includes intra-molecular screening, and U is the screened on-site Coulomb term in the crystal whereas V denotes the screened nearest neighbour parameter. All energies are in eV.

molecules a relative distance of $\vec{l}$ apart, i.e.

$$V_{\mathrm{bare}}^{\nu,\vec{l}} = \int d^3\vec{r}\,d^3\vec{r}'\ \frac{\rho_\nu^0(\vec{r})\rho_\nu^{\vec{l}}(\vec{r}')}{|\vec{r}-\vec{r}'|}\ , \tag{3}$$

where $\rho_\nu^{\vec{l}}(\vec{r}) = |\phi_\nu^{\vec{l}}(\vec{r})|^2$ and $\phi_\nu^{\vec{l}}(\vec{r})$ is the wave function of orbital ν at position $\vec{l}$. Obviously the local Coulomb integral, the Hubbard-U_{bare}, is given by $V_{\mathrm{bare}}^{\nu,\vec{0}} = U_{\mathrm{bare}}$. The bare parameters are, in general, too large since all screening effects are neglected. To calculate the on-site Coulomb parameter U_0 including intra-molecular screening we use (all-electron) density functional theory total energy calculations for different additional charges q on a single molecule. To obtain U_0 for HOMOs electrons are taken away and similarly for LUMOs electrons are added to the molecule. The Kohn-Sham DFT total energy consists of several contributions. It reads

$$E^{\mathrm{total}}[n] = \sum_{i=1} \varepsilon_i n_i - \int d^3\vec{r}\, V_{\mathrm{xc}} n(\vec{r}) - \frac{e^2}{2} \int d^3\vec{r}\,d^3\vec{r}'\ \frac{n(\vec{r})n(\vec{r}')}{|\vec{r}-\vec{r}'|} + E_{\mathrm{xc}}[n] + V_{\mathrm{ions}}\ , \tag{4}$$

where the ε_i are the Kohn-Sham eigenenergies and n_i the corresponding occupation numbers, V_{ions} denotes the ion-ion interaction.

The terms behave differently when subjected to a change in electron density. Charging up the molecule with q leads to a linear change in the occupation numbers n_ν for the orbital ν with energy ϵ_ν. The Hartree potential also has a linear contribution. This can be seen when substituting $\rho \rightarrow \rho + \delta\rho$, where $\delta\rho$ denotes the change due to the additional charge. Its contribution however is mainly quadratic. The effects of the exchange-correlation potential are usually small and therefore neglected. Thus, fitting the total energies for different additional charges to the function

$$E_{U_0^\nu}(q) = a_0 + a_1 q + U_0^\nu \frac{q^2}{2}\ , \tag{5}$$

yields the desired U_0 and a_0, a_1 as further fit parameters. a_0 should be about the energy for $E_{U_0^\nu}(0)$. a_1 captures the linear effects in q. The factor $1/2$ of the quadratic term stems from the factor $1/2$ in the Hartree potential in equation (4).

Similarly $V_0^{\nu,\vec{l}}$ is calculated. We consider two molecules with an additional charge of $q/2$ put on both of them. The total energy for different q is fitted to

$$E_{V_0^{\nu,\vec{l}}}(q) = 2E_{U_0^\nu}(q/2) + b_0 + b_1 q + V_0^{\nu,\vec{l}}\left(\frac{q}{2}\right)^2\ , \tag{6}$$
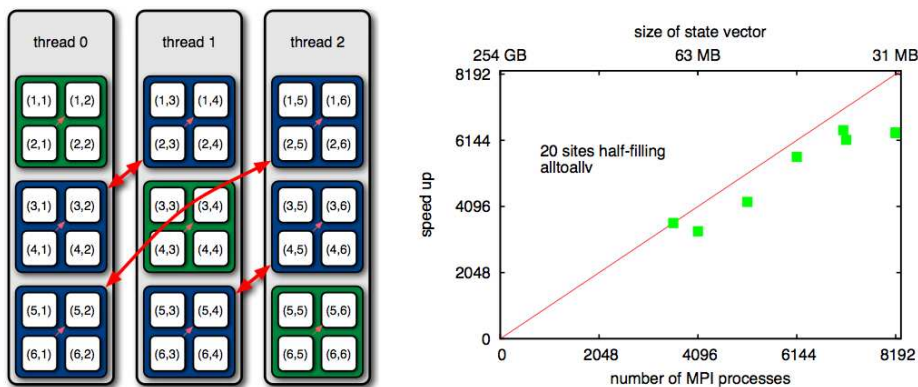
yielding $V_0^{\nu,\vec{l}}$.

Figure 2. (left) Transpose operation that makes memory access thread-local when calculating the operation of the Hamiltonian on the state-vector. The communication (red arrows) is realized by a call to `MPI_alltoall`, which is very efficiently implemented on BlueGene/L. The small pink arrows indicate the local operations needed to complete the matrix-transpose;(right) Speed-up of our Lanczos code on IBM Blue Gene/L JUBL in CO mode for 20 sites half-filled Hubbard model.

To also include the inter-molecular screening contribution requires calculations of the energy of an infinite lattice of molecules. We employ an electrostatic approach and represent the molecules by their polarizabilities. The polarizability tensor of the isolated molecules is calculated with DFT, by evaluating the dipole moments in homogeneous external fields along the principal axes and extracting the linear response. Regarding the molecules as point-polarizabilities we can calculate the fully-screened parameters[3] with the distributed dipole-approach. All parameters are compiled in table 1.

3   Computational Aspects

The key ingredient of the Lanczos algorithm, our eigenvalue solver, is the sparse matrix vector multiplication. Already for quite small systems this operation takes most of the execution time, and with increasing the size of the many-body vector it dominates even more. Thus it will be in the focus of our parallelization efforts. On shared memory systems this matrix-vector multiplication is embarrassingly simple but we are restricted to relatively small memories. To use the memory that is needed to reduce finite size effects, we had to find an efficient distributed memory implementation.

The kinetic energy term of the Hamiltonian (1) has non-diagonal terms and therefore leads to non-local memory access patterns. To obtain an efficient distributed memory implementation we use a simple yet important observation: As pointed out above, the kinetic energy term conserves spin. Thus, performing the up-electron hopping takes only different up-hopping configurations into account while the down-electron configuration remains unchanged. If we group all up configurations for a fixed down configuration together in a single thread this hopping can thus be carried out locally: for a fixed index $i_\downarrow$, all $i_\uparrow$ configurations follow and can be stored in a thread. We see, that this basis can be naturally indexed by a tuple $(i_\downarrow, i_\uparrow)$ instead of a global index We can therefore equivalently regard
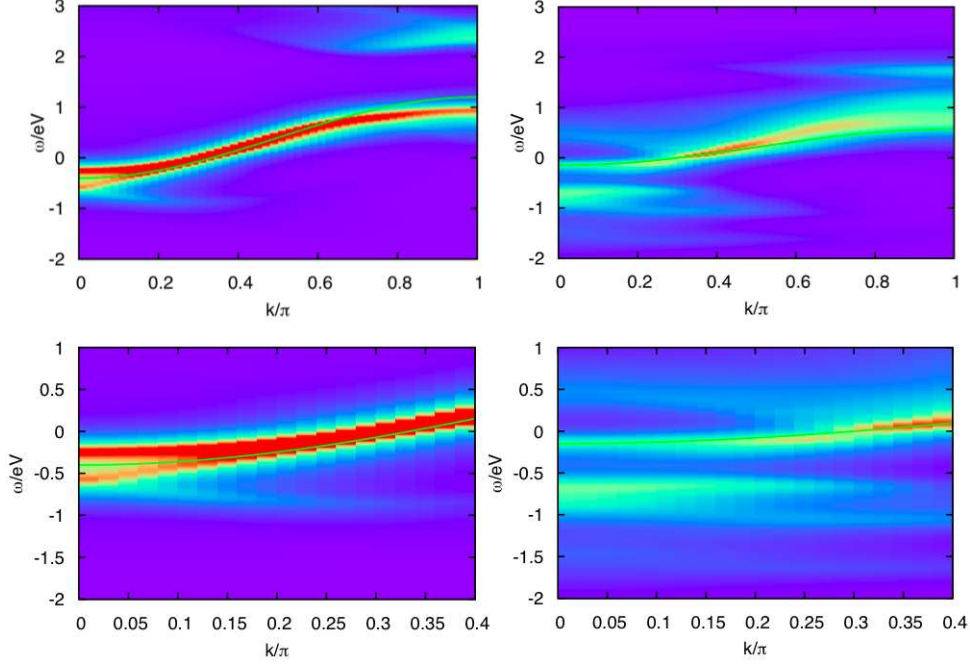
Figure 3. (first row) Angular-resolved spectral function obtained by CPT for a 20 sites TCNQ-like, i.e. six electrons of either spin, t-U Hubbard model with $U = 1.96$ eV, $t = 0.4$ eV (left) and t-U-V Hubbard model with $U = 1.7$ eV, $t = 0.18$ eV and $V = 0.9$ eV (right). The second row shows a magnification of the vicinity of the Γ point. In the t-U model we clearly observe signatures of spin-charge separation, whereas for the t-U-V model the lower branch is split. The green cosine shows the independent-particle band.

the vectors as matrices $v(i_\downarrow, i_\uparrow)$ with indices $i_\downarrow$ and $i_\uparrow$. Now it is easy to see that a matrix transpose reshuffles the data elements such that the down configurations are sequentially in memory and local to the thread. Therefore, the efficiency of the sparse matrix-vector multiplication rests on the performance of the matrix transpose operation. We implement it with MPI_Alltoall. This routine expects, however, the data packages which will be sent to a given process to be stored contiguously in memory. This does not apply to our case, since we would like to store the spin-down electron configurations sequentially in memory. Thus, the matrix is stored column wise. For MPI_Alltoall to work properly, we would have to bring the data elements in row-major order. This could be done by performing a local matrix transpose. The involved matrices are, however, in general rectangular, leading to expensive local-copy and reordering operations. We can avoid this by calling MPI_Alltoall for each column separately. After calling MPI_Alltoall for each column (red arrows in figure 2) only a local strided transposition has to be performed (small pink arrows) to obtain the fully transposed matrix or Lanczos vector.[5,6] The speed-up (figure 2) shows that collective communication is indeed very efficient on BlueGene/L.
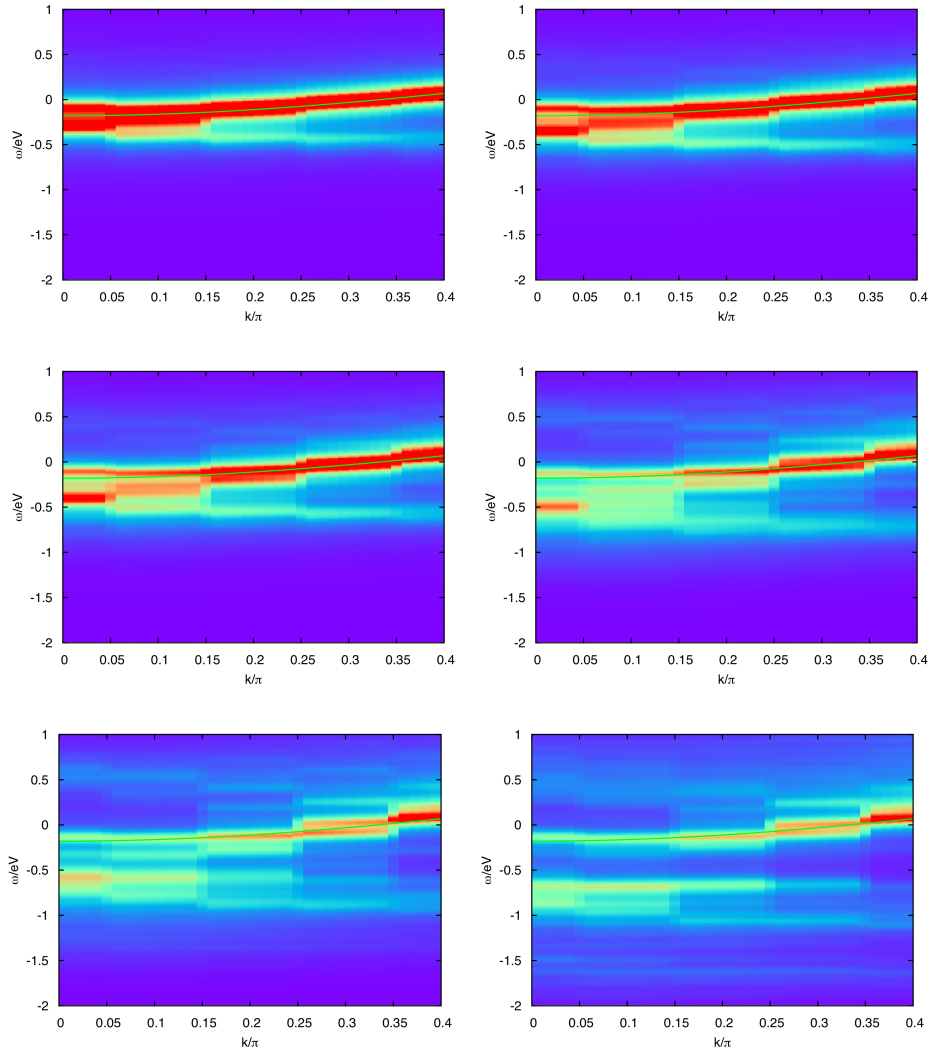
Figure 4. kCPT angular-resolved spectral functions close to the Γ point for 20 sites TCNQ-like Hubbard model with 6 electrons of either spin and different values of the nearest neighbour Coulomb repulsion $V = \{0.0, 0.1, 0.2, 0.4, 0.6, 0.9\}$eV ($U = 1.7$eV, $t = 0.18$eV). We clearly observe the increase in the splitting of the former holon and spinon branch with increasing values of V.

4 (k)Cluster Perturbation Theory and Spin-Charge Separation

Our parallel implementation of the Lanczos method enables us to efficiently calculate angular-resolved spectral functions for quite large systems. However, we still can have at most as many different momenta as we have sites. To resolve exciting physics like spin-charge separation we need, however, a higher resolution. A way to achieve this is cluster

perturbation theory (CPT).[7] The general idea is to solve a finite cluster with *open boundary conditions* exactly and then treat hopping between clusters in strong coupling perturbation theory, leading to an effectively infinite chain.

Figure 3 shows the angular-resolved spectral function for TCNQ in a CPT calculation for a 20 sites t-U Hubbard model. At the Γ-point we observe signatures of spin-charge separation: The electron dispersion splits into a holon and a spinon branch. These features are also observed in experiments. Usually the parameter set $U = 1.96$ eV, $t = 0.4$ eV has been used in the calculations since they fit the experiments fairly well. The parameter calculations, however, show that t should be smaller by a factor of more than two, but on the other hand the nearest neighbour interaction V should not be neglected since it is about half the value of U. We thus repeated the calculation with the realistic parameters derived above and observe that V effectively doubles the bandwidth. At the same time the spectral-weight of the holon-band spreads and the simple Luttinger liquid behaviour is lost.

To study this transition we need several calculations for different values of V. CPT calculations are, however, quite expensive. To generate the CPT plots about three Blue-Gene/L rack-days are needed: The calculation of the ground state is negligible and takes considerably less than half an hour on 2048 processors in VN mode on a BlueGene/L system. To calculate the Green's function for photoemission and inverse photoemission about 400 Green's functions each have to be calculated, where the former calculation takes a total of about 15 hours whereas the latter one takes about two days. We thus want to resort to a computationally less demanding, however, more finite-size effect prone method – the kCPT method. The key idea is to always keep translational symmetry by using periodic boundary conditions. Figure 4 shows how increasing V shifts apart the spectral features close to the Γ point.

References

1. W. Kohn, *Nobel Lecture: Electronic structure of matter: wave functions and density functionals*, Rev. Mod. Phys. **71**, 1253, 1999.
2. E. Koch and E. Pavarini, *Multiple Scales in Solid State Physics*, Proceedings of the Summer School on Multiscale Modeling and Simulations in Science 2007, Springer.
3. L. Cano-Cortés, A. Dolfen, J. Merino, J. Behler, B. Delley, K. Reuter, and E. Koch, *Coulomb parameters and photoemission for the molecular metal TTF-TCNQ*, Eur. Phys. J. B **56**, 173, 2007.
4. J.P. Perdew, K. Burke, and M. Ernzerhof, Phys. Rev. Lett. **77**, 3865, 1996.
5. A. Dolfen, *Massively parallel exact diagonalization of strongly correlated systems*, Diploma Thesis, RWTH Aachen, October 2006.
6. A. Dolfen, E. Pavarini, and E. Koch, *New Horizons for the Realistic Description of Materials with Strong Correlations*, Innovatives Supercomputing in Deutschland **4**, 16, Spring 2006.
7. D. Sénéchal, D. Perez, and M. Pioro-Ladrière, *Spectral Weight of the Hubbard Model through Cluster Perturbation Theory*, Phys. Rev. Lett. **84**, 522, 2000.
8. T. Maier, M. Jarrell, Th. Pruschke, M. Hettler, *Quantum Cluster Theories*, Rev. Mod. Phys **77**, 1027, 2005.